DOI: 10.5137/1019-5149.JTN.16940-16.3
Received: 05.01.2016 / Accepted: 28.03.2016
Published Online: 05.08.2016

Original Investigation

Vagal Ischemia Induced Lung Immune Component Infarct Following Subarachnoid Hemorrhage: An Experimental Study

Canan ATALAY[1], Betul GUNDOGDU[2], Mehmet Dumlu AYDIN[3]

[1]Ataturk University, Faculty of Medicine, Department of Anesthesiology, Erzurum, Turkey
[2]Ataturk University, Faculty of Medicine, Department of Pathology, Erzurum, Turkey
[3]Ataturk University, Faculty of Medicine, Department of Neurosurgery, Erzurum, Turkey

ABSTRACT

AIM: Neurogenic pulmonary edema (NPE) is the most serious complication of subarachnoid hemorrhage (SAH). As vagal nerves have vital roles in lung functions, vagal ischemia may have a causative role in the pathogenesis of NPE. We examined whether there was a relationship between vagal complex ischemia and lung immune complexes occupying the lymph node infarct in SAH.

MATERIAL and METHODS: Thirty-two rabbits were divided into three groups: Control (n=5), SHAM (n=5) and SAH group (n=22). SAH was created by autologous blood injection into the cisterna magna and followed-up for 3 weeks. Vasospasm index (VSI) was defined as the ratio of the lung lymph node arteries (LLNA) wall section (wall ring) surface to the lumen surface. Degenerated axon numbers of vagal nerves, neuron densities of the nodose ganglion (NG) and VSIs of LLNA were compared for all groups.

RESULTS: The mean degenerated vagal nerve axon density, neuron density of NG, and VSI of LLNA were 26±8/mm^2, 30±5/mm^3, and 0.777±0.048 in the control group; 1300±100/mm^2, 720±90/mm^3, and 1.148±0.090 in the animals with slight vasospasm (n=12); and 7300±530/mm^2, 5610±810/mm^3, and 1.500±0.120 in the animals with severe vasospasm (n=10), respectively.

CONCLUSION: Degenerated vagal axon and NG neuron density may be a causative factor in the development of LLNA vasospasm induced lymph node infarct in SAH. Lung lymph node infarct may be an important factor in the prognosis of NPE.

KEYWORDS: Subarachnoid hemorrhage, Vagal nerve, Lung lymph node infarct, Neurogenic pulmonary edema

INTRODUCTION

The lymph nodes are the most important integral part of the lung's immune system when coping with foreign bodies, metabolites and dangerous compounds. The pulmonary lymphatic system is involved in immune homeostasis and surveillance (14). Cholinergic pathways are localized in the lung lymphoid tissues, which play an important role in the modulation of neuronal metabolism and immunity in the lungs (9). The lungs are innervated by vagal, cervical sympathetic, and thoracic somatic nerves that are primarily responsible for the continuation of respiration reflexes (11). Sensory innervation of the respiratory tract is regulated primarily at the level of the nodose ganglion (NG) and pulmonary microganglia of the vagal nerves (34), glossopharyngeal nerves (GPN), and cervicothoracic spinal ganglia (32).

The respiratory and immunoregulatory roles of vagal nerve on the lungs (18) may be damaged (37) due to vagal nerve injury in subarachnoid hemorrhage SAH (6) and pulmonolymphatic vessel innervation deficiency resulting in lung immune defects (31). Hypoxia induces pulmonary vasoconstriction (32) and immune deficiency in the lungs (8). At the beginning of SAH, ischemic neurons of the vagal nerves generate uncontrollable parasympathetic discharges leading to lung edema associated with dilated lung lymph node arteries (LLNA) and increased vagal cholinergic activity, and consequently to cardiorespiratory hypertension (5,10). Neurogenic pulmonary edema (NPE)

qr code

Corresponding author: Mehmet Dumlu AYDIN
E-mail: nmda11@hotmail.com

in severe SAH is observed due to lacking parasympathetic stimulation of the lungs caused by uncontrollable LLNA vasospasm and lymphatic tissue infarct (21). Vagotomy blocks brain mediated fever and inflammation (19). Ischemic vagal injuries trigger pulmonary inflammation and infections. Alterations in NG following SAH have not been studied in the pathogenesis of lung lymph node infarct.

This experiment was carried out to determine correlation between the live and degenerated axon numbers of vagal nerves and neuron numbers of NG with lung lymph node arterial diameters following SAH. We theorized that the destruction of lymphatic components of the lungs is a major complication of SAH that has not been mentioned in the literature so far.

MATERIAL and METHODS

Experimental Protocol and Animals

The experimental protocol was approved by the Ethics Committee of Atatürk University, Medical Faculty. A total of 32 hybrid rabbits weighing an average of 3.7±0.3 kg at age of 1.5 years were used. Both the control and SHAM groups consisted of 5 rabbits. The remaining animals (n=22) were injected autologous blood into their cisterna magna and decapitated after 3 weeks of follow-up. Balanced injectable anesthetics were used in order to reduce the pain and mortality. After inducing anesthesia with isoflurane via a facemask, 0.2 ml/kg of the anesthetic combination (Ketamine HCl, 150 mg/1.5 ml and Xylazine HCl, 30 mg/1.5 ml; and distilled water, 1 ml) was subcutaneously injected prior to surgery. During the procedure, a dose of 0.1 ml/kg of the anesthetic combination was used when required. Autologous blood (1 ml) was taken from the auricular vein and injected using a 22-Gauge needle into the cisterna magna of animals in the SAH group over the course of 1 minute (Figure 1). In the SHAM group, 1 ml of serum physiologic was injected into the cisterna magna. The animals were followed for 20 days without any medical treatment and then sacrificed. The animals in the control group were remained intact. The brains and lungs were kept in 10% formalin solutions for retrograde histological examination.

Histopathological Procedures

All of the lungs and vagal nerves together with their ganglions were extracted bilaterally below the jugular foramens in order to estimate the axon density of the vagal nerves and the neuron density of the NG. The tissues were embedded in paraffin blocks longitudinally and horizontally for the former and the latter to observe all the roots during the histopathological examination. They were stained with hematoxylin & eosin (H&E), tri-chrome Masson (TCM), and terminal deoxynucleotidyl transferase dUTP nick end labeling (Tunel) stain. The Cavalieri method was used to evaluate the density of axons in the vagal nerve roots (12). The physical dissector method was used to evaluate the number of neurons in the NG. Two consecutive sections (dissector pairs) obtained from the tissue samples with named reference were mounted on each slide. Reference and look-up sections were reversed in order to double the number of dissector pairs without cutting new sections. The mean number of neuron density of nodose ganglions (NvGN) per mm^3 was estimated using the following formula as follows:

The mean numerical density of normal and degenerated neurons in the nodose ganglia (N_v/G_v) per cubic millimeter was estimated using the following formula:

$$N_v/G_v=\sum Q-/\sum Axd$$

Nv/Gv=∑Q–/∑Axd, where $\sum Q^{-}N$ is the total number of counted neurons appearing only in the reference sections, *d* is the section thickness, and *A* is the area of the counting frame. The most effective way of estimating $\sum A$ for the set of dissectors is using $\sum A = \sum Pa$, where $\sum P$ is the total number of counting set frame points and *a* is a constant area associated with the set point (12). The total number of neurons was calculated by multiplying the volume (mm^3) and the numerical density of neurons in each NG. The number of neurons in NG was counted for each animal (Table I).

The LLNAs were harvested from the longitudinal sections at the lymph node hilus level. To calculate vasospasm index (VSI), the surface of the LLNA was determined using cylindrical geometry. The LLNAs were cut 20 segments away from the

Table I: The Relationship Between the Degenerated Vagal Axon and Neuron Density and the Values of Pulmonary Artery Vasospasm Indices (VSI) are Summarised

Measurements	Vasospasm Levels		
	Normal	Slight	Severe
Degenerated axon density (per mm^2)	26±8	1300±100	7300±530
Degenerated ganglion density (neuron/mm^3)	30±5	720±90	5610±810
VSI	0.777±0.048	1.148±0.090	1.500±0.120

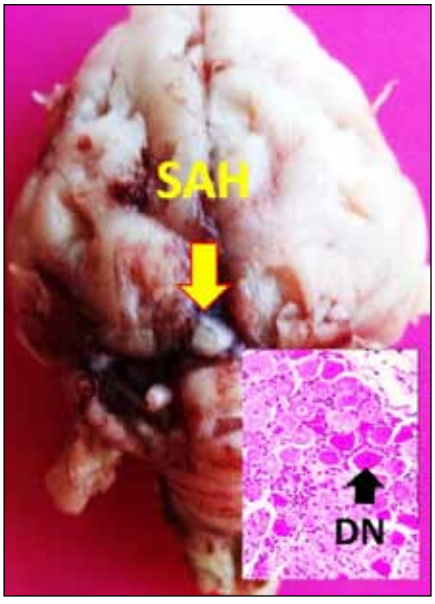

Figure 1: Gross anatomopathological appearance of a brain of an animal with SAH (A) and ischemic neurodegeration detected in the nodose ganglion with normal (NN) and degenerated (DN) neurons after SAH induction (LM, H&E, x4).

arising point of the main LLNA to the entering points of lymph nodes. Then, 20 subsequent histopathological sections with 5 µm intervals were cut (indicated by line a to u) to achieve representatively the mean external diameter and internal (luminal) diameters, external radius (R_e), and internal radius (r_i) (Figure 3A, B). The wall ring surface (S_1) was calculated using the following formula as follows:

$S_1 = \pi R_e^2 - \pi r_i^2$

The lumen surface (S_2) was calculated in similar algorithm, which was equal to πr_i^2. The VSI is the ratio of the S_1 to S_2. That is, it is equal to $\pi(R_e^2 - r_i^2)/ \pi r_i^2$, to $(R_e^2 - r_i^2)/r_i^2$ when simplified.

Data Analysis

Degenerated axon numbers of vagal nerves, neuron densities of NG, and VSI of the LLNA were compared using the Kruskal-Wallis and Mann-Whitney U tests (SPSS® for Windows v. 12.0, Chicago, IL). Differences were considered to be significant at $p< 0.005$.

RESULTS

Meningeal irritation signs, consciousness, convulsive attacks, fever, apnea, cardiac arrhythmia, and breathing difficulty were the typical clinical findings in premortal periods. Cardiac pulse, breath pulse, blood oxygen concentration were 250±30 per minute, 30±7 per minute, and 95±5% for normal animals and 140±40 per minute, 15±5 per minute, and 70±10% for animals affected by SAH at the beginning stage. There were remarkable electrocardiographic changes, including ST depression, ventricular extra-systoles, bigeminal pulses, QRS separation, and fibrillations. However, at the late phase of SAH, heart pulse increased to 330±30 per minute. The respiration rate was 20±4 bpm at the beginning, and 10 hours later, it increased to 40±9 bpm with severe tachypneic and apneic characteristics. The respiration frequency decreased to 15±5 per min (bradypnea) and respiration amplitude increased by 30% at the first hours of SAH. However, at the later stage, the respiration frequency increased (tachypnea), respiration amplitude decreased (30±8%), inspiration shortened, and expiration time was prolonged, which were accompanied by apnea-tachypnea attacks, diaphragmatic breath, and respiratory arrest.

Figure 1 illustrates gross anatomopathological appearance of the brain of a dead animal affected by SAH as well as ischemic neurodegeneration in NG with normal neurons (NN) and degenerated neurons (DN) upon SAH induction. Axonal and periaxonal slimming, axonal loss, and expanded interaxonal space were considered signs of axonal degeneration in histopathological examination of vagal nerves. These changes of vagal nerves were less severe in living animals affected by SAH (Figure 2A, B). Histological appearance of a normal lung tissue, lymph node (LN), bronchioles (Br), and pulmonary artery (PA) as well as LLNA in lymph node and VSI estimating method are shown in Figure 3. NG degeneration is shown in Figure 4A. The inner elastic membrane (IEM) was less convoluted and the luminal surface area was greater in the control and light vasospastic SAH groups. Moreover, narrowed LLNAs, convoluted IEM, edema in intima, shrunk endothelial cell shrinkage, and desquamation and endothelial cells loss were evident in the SAH groups (Figure 4B). Histological appearance of inflamed and degenerated mega lymph node of a lung with lymphatic infarct, hemorrhagic infiltrations in lymph node was associated with severe vagal degeneration, increased lymph node volume, blood collection in lymph node, and ruptured lymph nodes into bronchioles indicated lymphatic infarct is shown in Figure-4/Base. Severe hemorrhagic-neurogenic lung edema, lymph node degeneration (Blue stars/Figure 5/Base), severe inflamed and spastic LLNA (Figure 5A) and endothelial shrinkage, desquamation and intimal proliferation are seen (Figure 5B). In Figure 6/base, apoptotic lung tissues, spastic

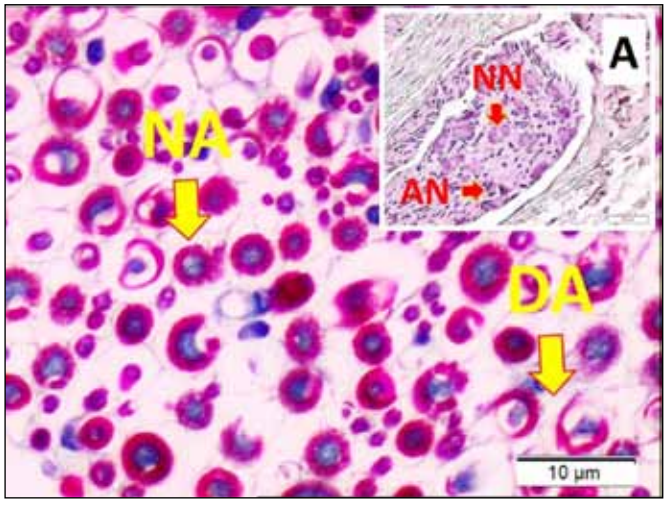

Figure 2: Normal (NA) and degenerated (DA) axons as well as normal (NN) and apoptotic (AN) neurons in the nodose ganglion of the vagal nerve associated with ischemic degeneration due to the SAH induction (LM, TCM, x10/**A**).

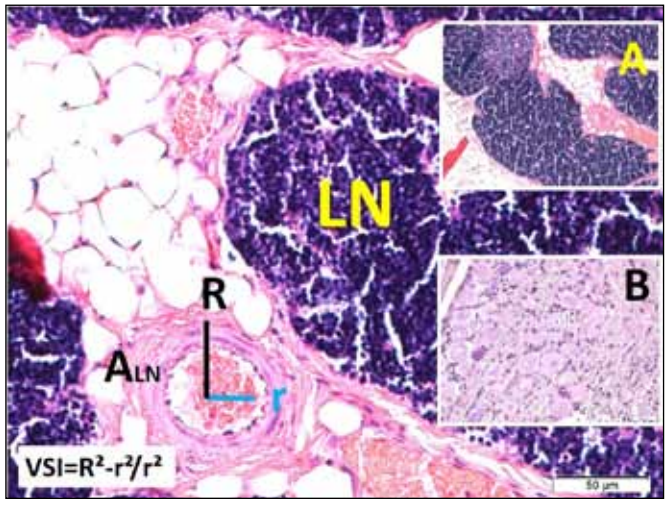

Figure 3: Histological appearance of normal lung tissue lymph node (LM, H&E, x4/**A**). Normal nodose ganglion neurons (LM, Tunel, x10/**B**) lymph node supplying artery of lymph node and VSI estimating method are shown of a normal rabbit (LNA/(LM, H&E, x10/Base).

degenerated LLNA (Figure 6A) and degenerated lymphatic vessels are seen (Figure 6B).

The mean VSI of LLNA, normal vagal nerve axon density, and neuron density of NG for the rabbit family was 0.777±0.048, 29700±8500 per mm^2, and NG10.230±1.010 per mm^3, respectively. The mean degenerated vagal nerve axon density, degenerated neuron density of NG, and VSI of LLNA were 26±8/mm^2, 30±5/mm^3, and 0.777±0.048 in the control group; 1300±100/mm^2, 720±90/mm^3, and 1.148±0.090 in the animals with slight vasospasm (n=12); and 7300±530/mm^2, 5610±810/mm^3, and 1.500±0.120 in the animals with severe vasospasm (n=10), respectively (Table I)

DISCUSSION

Developing vagal nerve root injury in SAH causes disruption of efferent and afferent vagal reflex pathways that regulate respiration. The GPN, other lower cranial nerves and upper cervical spinal nerves are injured as well. Disruption extends into the cervical spinal canal, aggravating the mortal effects of SAH. These result in alteration in breathing pattern and respiration arrest (33) through initiating the Hering-Breuer reflex (24). All neurons generate electrical impulse when they are exposed to ischemia. Ischemic vagal nerves induced by SAH generate uncontrollable parasympathetic discharges and lead to lung edema via dilated pulmonary arteries (10). Excessive discharge of vagal nerves may be responsible for increased cholinergic activity on the heart and heart dysfunctions at the beginning of SAH. Non-discharged ischemic vagal nerves cause heart rhythm variation and cardiac arrest in the late phase of subarachnoid hemorrhage (5). Meanwhile, ischemic vagal nerve roots are unable to drive the parasympathetic stimulation of the pulmonary arteries and heart. Bilateral vagal nerve stimulation causes bronchoconstriction (24). One of the other important causes of breathing disability at the beginning of SAH is bronchoconstriction resulting from ischemic vagal discharge (9). Ischemic vagal nerve root injury is involved in the development of respiratory arrhythmia and pulmonary injury with bronchospasm (5).

Respiratory organs are innervated by the vagal nerves, sympathetic nerves and the upper four or five thoracic somatic nerves. The vagal nerves play a role in the maintenance of respiration via regulating airways and pulmonary vessel resis-

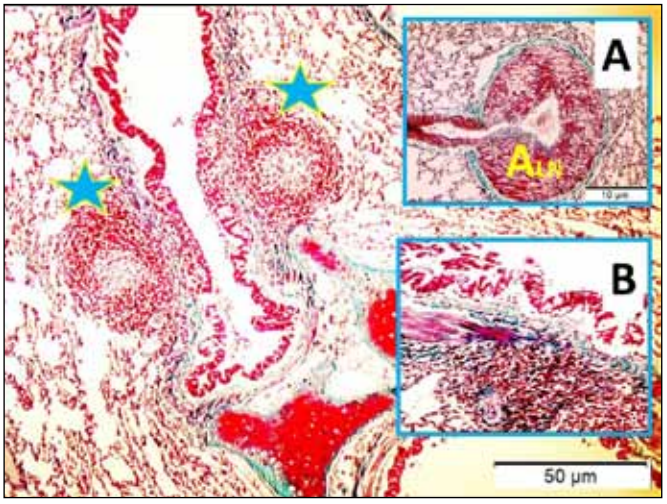

Figure 5: Histological appearance of destructed lung lymph node and thrombosed lymph node supplying artery (LM, TCM, x10/**A**) as well as hemorrhagic infiltrations in lymph node of a dead rabbit (LM, TCM, x4/**Base**) and magnified form of inflamed LLNA (LM, TCM, x20/**B**) due to severe vagal degeneration.

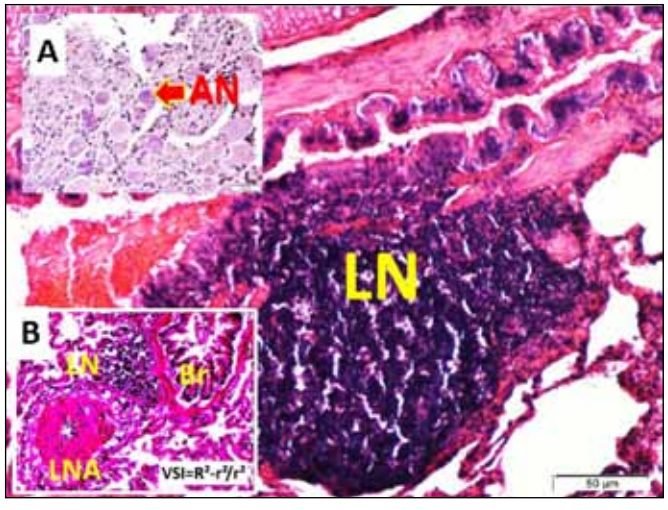

Figure 4: Histological appearance of inflamed and degenerated mega lymph node of a lung with lymphatic infarct (LM, H&E, x10/**Base**). NG of vagal nerve with apoptotic neurons (AN) (LM, Tunel, x10/**A**). Ultimately spastic lymph node supplying artery (LNA) with contracted smooth muscle cells and spastic bronchiole associated with neurogenic lung edema due to the SAH induction (LM, H&E, x10/**B**).

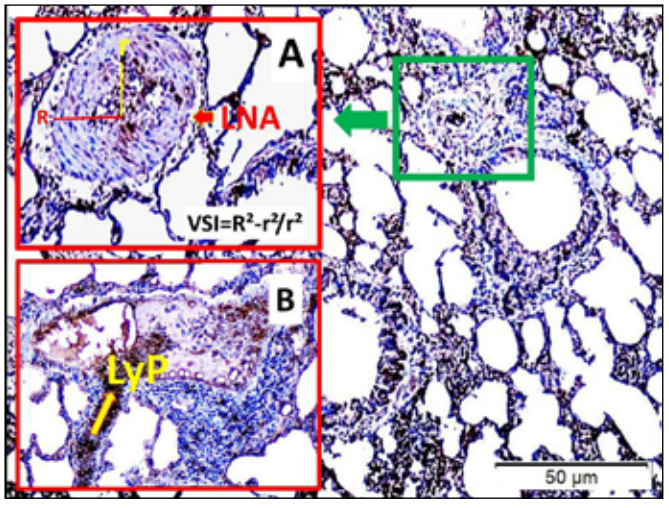

Figure 6: Histological appearance of lung of a severe neurogenic lung edema (LM, Tunel, x4/**Base**). Spastic LLNA with apoptotic endothelium, smooth muscle cells, and narrowed lumen with VSI formula (LM, Tunel, x20/**A**). Thrombosed lumen (yellow arrow) and massive lymphatic infarct with lymphatic product (LyP) accumulation in a lymphatic lacunae (LM, Tunel, x4/**B**).

tance, pulmonary pressure, the Hering-Breuer reflex, blood pH, respiration and heart rhythm coordination, and lung metabolism and immunity (36). Irritant receptors of the vagal nerves regulate breath rhythm via bronchial and tracheal constriction and slowing the heart rate (13). Cholinergic neurons, inhibitory noradrenergic neurons, and somatosensitive neurons that form pulmonary plexuses are also in charge of controlling the calibers of conducting airways, diameter of pulmonary vasculature, volume of respiratory units and activity of bronchial glands and respiration reflexes (11,17,20).

Vagal nerve injury causes laryngopharyngeal muscle paralysis, tracheobronchial distortions, reflex vagal bradycardia, and bradypnea (29). Its blockage eliminates both the frequency and amplitude of spontaneous breaths (24), which is similar to irreversible axonal injury of the vagal nerve in late stage SAH (4,5). The Hering-Breuer reflex may also be abolished during acutely developed cerebral ischemia that could be restored by recovery of ischemic cerebral processes (7). Bilateral vagal nerve stimulation causes bronchoconstriction (24) that is one of the factors contributing to breathing disability at the beginning of SAH linked to ischemic vagal discharge (1,9).

In SAH, through damaging brainstem and cranial nerve injuries (26), respiration muscles are paralyzed and breathing reflexes. All autonomic and somatic nerves control the calibers of the conducting airways and pulmonary blood vessels, the volume of respiratory units, the activity of bronchial glands and respiration reflexes (11). The somatosensitive motor nerves surround the respiration muscles, pleural and thoracic surfaces (23). Skeletal muscle proprioceptors of the somatosensitive nerves play a major role in the conscious continuation of respiration (28). The origins of sensory innervation of the lower respiratory tract are the nodose and jugular ganglia of the vagal nerve, and spinal ganglia at levels C2-C6 and T1-T6 ganglia (30). The sensory innervation of the rat lungs originates from the dorsal root ganglia (32). Stimulating the cervical sympathetic trunk in the caudal direction induces vasoconstriction in the bronchial and pulmonary vasculature (15). Infected ganglions of the olfactory, vagal, trigeminal nerves facilitate destruct lung functions and decrease lung immunity (1,27). Impulses of chemoreceptors are conveyed by GPN and vagal nerve fibers to the respiration centers (24). Vagal pulmonary myelinated afferents innervate lung tissue. Pulmonary neurons of vagal nerves are localized in NG (39). These afferent fibers sustain conduction velocity, neuropeptide content, sensitivity to chemical and mechanical stimuli, as well as evoked reflex responses of the lungs (22). Together with the vagal and spinal sensory fibers, sympathetic fibers form the pulmonary plexus that regulates lung functions via microganglia (34). The role of vagal nerve injury on the lung immune compartments in the SAH is related to cardiac arrest caused by ischemic nodosal and petrosal ganglia injuries of the vagal nerves.

The lung is invested with a rich supply of lymphatics and lymph nodes. The lymph nodes are an integral common part of the immune system of lungs dealing with external foreign substances, chylomicrons, lymphatic and metabolic particles, tumoral metastases and bacteria. Hyperthrophied hilar and intrapulmonary lymph nodes are frequently seen in serious lung disease. The lymphatic drainage into the lungs is via the thoracic ducts. The thoracic duct can be accepted as a canal conveying lymphatic products into the lungs. The lymphatic system of the lungs and the lymphatic vasculature have a major role in body homeostasis and immune surveillance and in the pathogenesis of lung disease (13, 31). The cholinergic anti-inflammatory pathway is a neurophysiological mechanism that regulates the immune system of lungs (16). Cholinergic pathways localized in the lung lymphoid tissues play a major role in general lung metabolism and neuro-immunomodulation (9,38). The immunoregulatory role of the vagal nerve on the lungs may be damaged secondary to vagal nerve injury, and the respiration rhythm may be disturbed due to lung inflammation (18). The early stress responses to hemorrhagic shock, trauma, and endotoxicosis are associated with an early pro-inflammatory response characterized by increased lymphocyte accumulation in the lungs and included apoptosis in the injured lung tissue (25).

Neurogenic pulmonary edema (NPE) is a fatal complication of SAH. Chylomicron metabolism may be disturbed in NPE and leakage of chylomicrons into the systemic circulation may be facilitated via the destroyed lung barrier in SAH, leading to cerebral fat embolism. (6). Not only chylomicrons but also other metabolic products, destructed tissue particles, infectious agents and even tumor cells are reported to be transported into lungs via the thoracic ducts. Indeed, systemic lipid embolism may not occur unless bone fractures lead to pulmonary injury (6). Thoracic duct ligation could prevent lungs from thoracic trauma and fat embolism (2,3).

There are no quantitative studies on the response of the LLNA diameter to the changes in living and degenerated neuron numbers of vagal nerves and NG. Changes in NG have not been studied to elucidate the relationship between SAH and lung lymph node infarct. SAH resulted in afferent and efferent vagal nerve complex ischemia at the brainstem due to vagal nerve root-supplying arteries' vasospasm. Degenerated vagal ganglions' neuron density may play major roles in the development of pulmonary LLNA vasospasm. The degenerated neuron density of vagal ganglia and axon densities were less in animals that experienced slight LLNA vasospasm, whereas the degenerated axon and neuron densities of vagal complex were higher in animals that experienced severe LLNA vasospasm.

■ CONCLUSION

This study showed that vagal nerve axonal injury and neuronal degeneration of NG correlated with LLNA vasospasm and lymph node infarct. From a clinical standpoint, the LLNA vasospasm and lymph node infarct may be related with NPE and vagal nerve stimulation could be a treatment method in pulmonary edema. Parasympathetic vasodilatory impulses of vagal nerves have major roles on the continuation of lung circulation within the normal limits. Ischemic injury of vagal nerve complexes induced by SAH can block the parasympathetic controls on the lungs and heart. Vagal nerve network degeneration leads indirectly to increased

sympathetic hyperactivity. Decreased parasympathetic and increased sympathetic impulses trigger the development of massive lung edema and lung immune deficiency and deplete the heart reserves. In brief, subcutaneous vagal nerve blockage may be useful at the beginning of SAH, whereas the vagal nerve stimulation or sympathetic blockage may be useful at the late phase of SAH.

REFERENCES

1. Auais A, Adkins B, Napchan G, Piedimonte G: Immunomodulatory effects of sensory nerves during respiratory syncytial virus infection in rats. Am J Physiol Lung Cell Mol Physiol 285:105-113, 2003
2. Aydin MD, Akçay F, Aydin N, Gündogdu C: Cerebral fat embolism: Pulmonary contusion is a more important etiology than long bone fractures. Clin Neuropathol 24:86-90,2005
3. Aydin MD, Eroglu A, Gundogdu C, Turkyilmaz A, Altas S, Aydin N: The preventive role of thoracic duct ligation on cerebral fat embolism in lung injury: An experimental study. Med Sci Monit 14:256-260,2008
4. Aydin MD, Eroglu A, Turkyilmaz A, Erdem AF, Alici HA, Aydin N, Altas S, Unal B: The contribution of chemoreceptor-network injury to the development of respiratory arrest following subarachnoid hemorrhage. EAJM 42:47-52, 2010
5. Aydin MD, Kanat A, Yilmaz A, Cakir M, Emet M, Cakir Z, Aslan S, Altas S, Gundogdu C: The role of ischemic neurodegeneration of the NG on cardiac arrest after subarachnoid hemorrhage: An experimental study. Exp Neurol 230:90-95, 2011
6. Aydin MD, Kotan D, Aydin N, Gundogdu C, Onder A, Akcay F: Mechanism of cerebral fat embolism in subarachnoid hemorrhage: An experimental study. Neuropathology 26:544-549, 2006
7. Aydin MD, Ozkan U, Gundogdu C, Onder A: Protective effect of posterior cerebral circulation on carotid body ischemia. Acta Neurochir 144:369-372, 2002
8. Cairns RA, Hill RP: Acute hypoxia enhances spontaneous lymph node metastasis in an orthotopic murine model of human cervical carcinoma. Cancer Res 64:2054-2061, 2004
9. Cavallotti C, Tonnarini G, D'Andrea V, Cavallotti D: Cholinergic staining of bronchus-associated lymphoid tissue. Neuroimmunomodulation 12:141-145, 2005
10. Costa C, Tozzi A, Luchetti E, Siliquini S, Belcastro V, Tantucci M, Picconi B, Ientile R, Calabresi P, Pisani F: Electrophysiological actions of zonisamide on striatal neurons: Selective neuroprotection against complex I mitochondrial dysfunction. Exp Neurol 221:217-224, 2010
11. Crapo JD, Barry BE, Czehr P, Bachofen M, Weibel ER: Cell number and cell characteristics of the normal human lung. Am Rev Respir Dis 126:332-333, 1982
12. Cruz-Orive LM, Weibel ER: Recent stereological methods for cell biology: A brief survey. Am J Physiol 258: L148-156, 1990
13. Dehkordi O, Rose JE, Balan KV, Kc P, Millis RM, Jayam-Trouth A: Neuroanatomical relationships of substance P-immunoreactive intrapulmonary C-fibers and nicotinic cholinergic receptors. J Neurosci Res 87:1670-1678, 2008
14. El-Chemaly S, Pacheco-Rodriguez G. Ikeda Y, Malide D, Moss J: Lymphatics in idiopathic pulmonary fibrosis: New insights into an old disease. Lymphat Res Biol 7:197-203, 2009
15. Franco-Cereceda A, Matran R, Alving K, Lundberg JM: Sympathetic vascular control of the laryngeo-tracheal, bronchial and pulmonary circulation in the pig: Evidence for non-adrenergic mechanisms involving neuropeptide Y. Acta Physiol Scand 155:193-204, 1995
16. Fuller SD, Freed AN: Partitioning of pulmonary function in rabbits during cholinergic stimulation. J Appl Physiol 78:1242-1249, 1995
17. Gaspari RJ, Paydarfar D: Respiratory failure induced by acute organophosphate poisoning in rats: Effects of vagotomy. Neurotoxicology 30:298-304, 2009
18. Goehler LE, Erisir A, Gaykema RP: Neural-immune interface in the rat area postrema. Neuroscience 140:1415-1434, 2006
19. Hansen MK, Nguyen KT, Goehler LE, Gaykema RP, Fleshner M, Maier SF, Watkins LR: Effects of vagotomy on lipopolysaccharide-induced brain interleukin-1beta protein in rats. Auton Neurosci 85:119-126, 2000
20. Ikomi F, Kousai A, Ono N, Ohhashi T: Electrical stimulation-induced alpha 1- and alpha 2-adrenoceptors-mediated contractions of isolated canine lymph nodes. Auton Neurosci 96: 85-92, 2002
21. Komotar RJ, Zacharia BE, Valhora R, Mocco J, Connolly ES Jr: Advances in vasospasm treatment and prevention. J Neurol Sci 261:134-142, 2007
22. Kwong K, Carr MJ, Gibbard A, Savage TJ, Singh K, Jing J, Meeker S, Undem BJ: Voltage-gated sodium channels in nociceptive versus non-nociceptive nodose vagal sensory neurons innervating guinea pig lungs. J Physiol 586:1321-1336, 2008
23. Lambert E, Jun Dux, Percy E, Lambert G: Cardiac response to norepinephrine and sympathetic nerve stimulation following experimental subarachnoid hemorrhage. J Neurol Sci 198:43-50, 2002
24. Matsumoto S, Takeda M, Saiki C, Takahashi T, Ojima K: Vagal block diminishes both the frequency and amplitude of spontaneous breaths and vagal reactivity increases peripheral airway resistance during inspiration. Lung 175:175-186, 1997
25. Molina PE: Noradrenergic inhibition of TNF upregulation in hemorrhagic shock. Neuroimmunomodulation 9:125-133, 2001.
26. Morga R, Czepko R, Dembińska-Kieć A, Danilewicz B: Assessment of the haemostatic system in patients surgically treated for ruptured cerebral aneurysm. Neurol Neurochir Pol 41:296-305, 2007
27. Park CH, Ishinaka M, Takada A, Kida H, Kimura T, Ochiai K, Umemura T: The invasion routes of neurovirulent A/Hong Kong/483/97 (H5N1) influenza virus into the central nervous system after respiratory infection in mice. Arch Virol 147:1425-1436, 2002
28. Prabhakar NR, Jacono FJ: Cellular and molecular mechanisms associated with carotid body adaptations to chronic hypoxia. High Alt Med Biol 6:112-120, 2005
29. Ryan S, McNicholas WT, O'Regan RG, Nolan P: Effect of upper airway negative pressure and lung inflation on laryngeal motor unit activity in rabbit. J Appl Physiol 92:269-278, 2002

30. Sakr YL, Lim N, Amaral AC, Ghosn I, Carvalho FB, Renard M, Vincent JL: Relation of ECG changes to neurological outcome in patients with aneurysmal subarachnoid hemorrhage. Int J Cardiol 96:369-373, 2004
31. Seyama K, Kumasaka T, Kurihara M, Mitani K, Sato T: Lymphangioleiomyomatosis: A disease involving the lymphatic system. Lymphat Res Biol 1:21-31, 2010
32. Springall DR, Cadieux A, Oliveira H, Su H, Royston D, Polak JM: Retrograde tracing shows that CGRP-immunoreactive nerves of rat trachea and lung originate from vagal and dorsal root ganglia. J Auton Nerv Syst 2:155-166, 1987
33. Stevens RD, Nyquist PA: The systemic implications of aneurysmal subarachnoid hemorrhage. J Neurol Sci 261:143-156, 2007
34. Taylor SM, Pare PD, Schellenberg RR: Cholinergic and nonadrenergic mechanisms in human and guinea-pig airways. J Appl Physiol 56:958-965, 1984
35. Vaughan DJ, Brogan TV, Kerr ME, Deem S, Luchtel DL: Contributions of nitric oxide synthase isozymes to exhaled nitric oxide and hypoxic pulmonary vasoconstriction in rabbit lungs. Am J Physiol Lung Cell Mol Physiol 28:834-843, 2003
36. Voelkel NF, Quaife RA, Leinwand LA, Barst RJ, McGoon MD, Meldrum DR, Dupuis J, Long CS, Rubin LJ, Smart FW, Suzuki YJ, Gladwin M, Denholm EM, Gail DB: Right ventricular function and failure: Report of a National Heart, Lung, and Blood Institute working group on cellular and molecular mechanisms of right heart failure. Circulation 114:1883-1891, 2006
37. Wang DW, Zhou RB, Yao YM: Role of cholinergic anti-inflammatory pathway in regulating host response and its interventional strategy for inflammatory diseases Chin J Traumatol 12:355-364, 2009
38. Wong GK, Wong R, Mok V, Wong A, Poon WS: Natural history and medical treatment of cognitive dysfunction after spontaneous subarachnoid haemorrhage: Review of current literature with respect to aneurysm treatment. J Neurol Sci 299:5-8, 2010
39. Zhang G, Lin RL, Wiggers M, Snow DM, Lee LY: Altered expression of TRPV1 and sensitivity to capsaicin in pulmonary myelinated afferents following chronic airway inflammation in the rat. J Physiol 586:5771-5786, 2008